Strong coupling of in-plane propagating plasmon modes and its control

Sachin Kasture,[1] Prasanta Mandal,[1,2] S. Dutta Gupta,[3] and Achanta Venu Gopal[1*]

[1]*DCMPMS, Tata Institute of Fundamental Research, Homi Bhabha Road, Mumbai 400005, India*
[2]*Present Address: Department of Physics, IIT, Kanpur, 208016, India*
[3]*School of Physics, University of Hyderabad, Hyderabad 500046, India*
[*]*achanta@tifr.res.in*

Abstract: We show anti-crossings due to strong in-plane coupling of grating excited propagating plasmon modes in dielectric-metal-dielectric structure with 2D dielectric pattern on top. Grating coupled propagating plasmon modes along with their complete dispersion in the measurement range and all different sample orientations are calculated first. Further a coupled mode theory is presented for the specific geometry presented here. Experimentally measured anti-crossing widths are compared with those calculated by coupled mode theory. It is shown that the coupling strength of the plasmon modes and thus the anti-crossing width can be controlled by the orientation of the sample.

OCIS codes: (240.6680) Optics at surfaces; (240.1485) Optics at surfaces.

References and links

1. L. Novotny, "Strong coupling, energy splitting, and level crossings: A classical perspective," Am. J. Phys. **78**(11), 1199–1202 (2010).
2. R. M. Stevenson, V. N. Astratov, M. S. Skolnick, D. M. Whittaker, M. Emam-Ismail, A. I. Tartakovskii, P. G. Savvidis, J. J. Baumberg, and J. S. Roberts, "Continuous wave observation of massive polariton redistribution by stimulated scattering in semiconductor microcavities," Phys. Rev. Lett. **85**(17), 3680–3683 (2000).
3. E. A. Stinaff, M. Scheibner, A. S. Bracker, I. V. Ponomarev, V. L. Korenev, M. E. Ware, M. F. Doty, T. L. Reinecke, and D. Gammon, "Optical signatures of coupled quantum dots," Science **311**(5761), 636–639 (2006).
4. D. Sarid, R. T. Deck, and J. J. Fasano, "Enhanced nonlinearity of the propagation constant of a long-range surface-plasma wave," J. Opt. Soc. Am. **72**(10), 1345–1347 (1982).
5. W. R. Holland and D. G. Hall, "Surface-plasmon dispersion relation: Shifts induced by the interaction with localized plasma resonances," Phys. Rev. B **27**(12), 7765–7768 (1983).
6. S. D. Gupta, G. V. Varada, and G. S. Agarwal, "Surface plasmons in two-sided corrugated thin films," Phys. Rev. B Condens. Matter **36**(12), 6331–6335 (1987).
7. K. F. MacDonald, Z. L. Samson, M. I. Stockman, and N. I. Zheludev, "Ultrafast active plasmonics," Nat. Photonics **3**(1), 55–58 (2009).
8. Y. Chu and K. B. Crozier, "Experimental study of the interaction between localized and propagating surface plasmons," Opt. Lett. **34**(3), 244–246 (2009).
9. G. S. Agarwal, S. Dutta Gupta, "Interaction between surface plasmons and localized plasmons," Phys. Rev. B Condens. Matter **32**(6), 3607–3611 (1985).
10. W. L. Barnes, W. A. Murray, J. Dintinger, E. Devaux, and T. W. Ebbesen, "Surface plasmon polaritons and their role in the enhanced transmission of light through periodic arrays of subwavelength holes in a metal film," Phys. Rev. Lett. **92**(10), 107401 (2004).
11. A. Christ, T. Zentgraf, S. G. Tikhodeev, N. A. Gippius, O. J. F. Martin, J. Kuhl, and H. Giessen, "Interaction between localized and delocalized surface plasmon polariton modes in a metallic photonic crystal," Phys. Status Solidi **243**(10), 2344–2348 (2006) (b).
12. Z. Chen, I. R. Hooper, and J. R. Sambles, "Grating-coupled surface plasmon polaritons and waveguide modes in a silver-dielectric-silver structure," J. Opt. Soc. Am. A **24**(11), 3547–3553 (2007).
13. H. Gao, J. Henzie, M. H. Lee, and T. W. Odom, "Screening plasmonic materials using pyramidal gratings," Proc. Natl. Acad. Sci. U.S.A. **105**(51), 20146–20151 (2008).
14. A. Ghoshal, I. Divliansky, and P. G. Kik, "Experimental observation of mode-selective anticrossing in surface-plasmon-coupled metal nanoparticle arrays," Appl. Phys. Lett. **94**(17), 171108 (2009).
15. J. Li, H. Lu, J. T. K. Wan, and H. C. Ong, "The plasmonic properties of elliptical metallic hole arrays," Appl. Phys. Lett. **94**(3), 033101 (2009).
16. A. Christ, S. G. Tikhodeev, N. A. Gippius, J. Kuhl, and H. Giessen, "Waveguide-plasmon polaritons: Strong coupling of photonic and electronic resonances in a metallic photonic crystal slab," Phys. Rev. Lett. **91**(18), 183901 (2003).

#186524 - $15.00 USD Received 7 Mar 2013; revised 16 May 2013; accepted 16 May 2013; published 23 May 2013

17. H. Raether, *Surface Plasmons on Smooth and Rough Surfaces and on Gratings* (Springer-Verlag, 1986).
18. S. D. Gupta, "Theoretical study of plasma resonance absorption in conical diffraction," J. Opt. Soc. Am. B **4**(11), 1893–1898 (1987).
19. S. Kasture, P. Mandal, A. Singh, A. Ramsay, A. S. Vengurlekar, S. Dutta Gupta, V. Belotelov, and A. Venu Gopal, "Near dispersion-less surface plasmon polariton resonances at a metal-dielectric interface with patterned dielectric on top," Appl. Phys. Lett. **101**(9), 091602 (2012).
20. S. G. Romanov, N. Vogel, K. Bley, K. Landfester, C. K. Weiss, S. Orlov, A. V. Korovin, G. P. Chuiko, A. Regensburger, A. S. Romanova, A. Kriesch, and U. Peschel, "Probing guided in a monolayer colloidal crystal on a flat metal film," Phys. Rev. B **86**(19), 195145 (2012).
21. M. López-García, J. F. Galisteo-López, A. Blanco, J. Sánchez-Marcos, C. López, and A. García-Martín, "Enhancement and directionality of spontaneous emission in hybrid self-assembled photonic-plasmonic crystals," Small **6**(16), 1757–1761 (2010).
22. H. Kogelnik and C. V. Shank, "Coupled-wave theory of distributed feedback lasers," J. Appl. Phys. **43**(5), 2327–2335 (1972).
23. R. Daendliker, "Coupled waves: A powerful concept in modern optics," SPIE Proc. Fifth International Topical Meeting on Education and Training in Optics **3190,** 279–288 (1997).
24. A. Kolomenskii, S. Peng, J. Hembd, A. Kolomenski, J. Noel, J. Strohaber, W. Teizer, and H. Schuessler, "Interaction and spectral gaps of surface plasmon modes in gold nano-structures," Opt. Express **19**(7), 6587–6598 (2011).
25. S. A. Maier, *Plasmonics: Fundamentals and Applications* (Springer, 2007).
26. J. M. Liu, *Photonic Devices* (Cambridge University, 2005).

1. Introduction

Strong coupling of polariton modes results in anti-crossings or avoided crossings in the dispersion plots and are studied in excitonic systems like exciton-photon coupling in cavities and exciton-exciton coupling in coupled quantum dots [1–3]. In the context of plasmons, coupled plasmons are studied where the coupling is between localized (particle) plasmons and propagating plasmons and coupling induced changes in dispersion in planar and corrugated structures [4–8]. In various sub-wavelength structures, these coupled localized and propagating plasmons are studied for basic physics as well as for different applications [9–16]. Also, in metal-dielectric-metal or dielectric-metal-dielectric structures when the middle layer is thin enough, coupling between plasmons at the top and bottom interfaces results in splitting of the modes to symmetric (short range) and anti-symmetric (long range) plasmon modes [17]. The general case of surface plasmon polariton (SPP) excitation in 1-d system when the grating vector is not contained in the plane of incidence has also been considered [18]. To our knowledge, there is no report on in-plane coupled propagating plasmons. We have recently shown grating coupled plasmon modes in dielectric-metal-dielectric layer structure with 2D dielectric grating on top and conditions under which near dispersionless plasmon modes can be excited in such structures [19]. Such excitation geometry would allow the coupling of in-plane propagating plasmons. In this paper we report on strong coupling of in-plane propagating plasmons at the unpatterned dielectric-metal interface originating due to the 2D grating structure on the top in the non-conical excitation geometry. In addition, we show that the coupling strength and thus the anti-crossing gap (split) width can be controlled. We give a model based on coupled mode theory to calculate the anti-crossing width.

2. Sample fabrication and measurement geometry

Samples studied have dielectric-metal-dielectric layer structure with 2D air holes in dielectric pattern on top. On quartz substrates, 50nm Gold was deposited by sputtering followed by spin coating of Shipley's S1805 photoresist on top. By interference lithography shallow 2D gratings of air holes in resist with depth of air holes of about 60 nm were prepared. There is an unpatterned resist of 400 nm thickness on the Gold layer constituting the top dielectric layer above the metal film. AFM and SEM images showed 2D air hole pattern is of rectangular lattice with periods 610 nm (a_x) and 625 nm (a_y) in the two orthogonal directions. The fill factors (air to dielectric ratio) are 0.65 and 0.7 in x and y directions, respectively. Figure 1 shows the schematic of the sample along with the measurement geometry and the SEM image. Further details about the structure are in Ref.19 and references therein. When the azimuthal angle is, $\varphi = 0°$, for TM polarized incident light launched in the plane perpendicular to the 2D pattern, the electric field component has finite component along a_x

#186524 - $15.00 USD Received 7 Mar 2013; revised 16 May 2013; accepted 16 May 2013; published 23 May 2013

which excites the SPPs. Similarly, for φ = 90° the finite electric field component along a_y excites the SPPs. Angle θ is the launch angle in the plane perpendicular to the XY-plane.

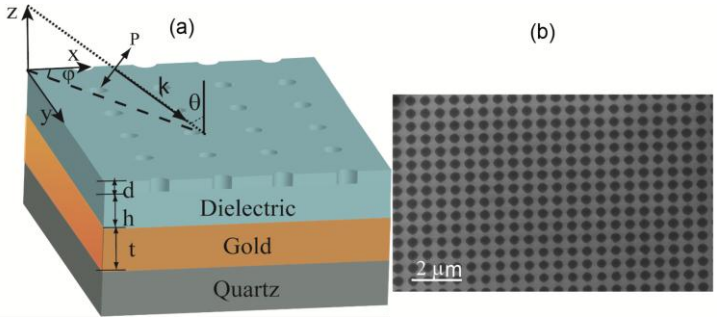

Fig. 1. (a) Shown is the schematic of the sample structure with dielectric-metal-dielectric layers having a 2-D air hole pattern in the top dielectric. Top dielectric is S1805 photoresist. Launch angle θ with respect to k and the azimuthal (in-plane) angle φ are shown. Various parameters such as the air hole depth (d), height of top unpatterned dielectric (h) and the thickness of the gold layer (t) are also marked. (b) SEM image of the sample.

3. Experimental results

Angle resolved transmission measurements are performed with the launch angle varied from –25° to + 25° range with 0.3° step. A 100 W halogen lamp is used as white light source (400-1000 nm wavelength range) and the output is collimated using a combination of apertures and lenses to have <0.3° divergence. Transmission spectra are recorded using a fiber spectrometer with 0.1nm spectral resolution.

Figure 2 shows the measured dispersion for three different angles φ. The data is normalized with that measured in sample with unpatterned top dielectric so that the dielectric loaded SPPs and/or waveguide modes are normalized to unity and thus do not contribute to the data presented here. It may, any case, be noted that the slab waveguide modes for this particular structure are expected at 526 nm (1,0), 460 nm (1,1), and 530 nm (0,1) while the (1,2) and (0,2) modes are out of range of the experimental wavelength range.

In addition to the propagating plasmons and the waveguide modes, hybrid photonic-plasmonic modes are also reported in structures with unpatterned dielectric layer or patterned dielectrics (photonic crystals) on metal layers [20, 21]. For the pattern under consideration, there are no photonic bandgap regions in the wavelength range of interest. Like in our recent report, we calculated all possible grating coupled propagating plasmon modes and their dispersion for all measured azimuthal angles [19]. Good match between the measured and calculated dispersion of all measured modes including pure grating modes can be seen in Fig. 2. It may be noted that Fig. 2 shows the SPP dispersion in grey scale plot thus the white regions show dips in the transmission spectra corresponding to plasmon excitation. Dashed lines are the fits based on a model that calculates the grating allowed propagating plasmon modes at the three layer structure [19]. Different SPP modes are labeled by $(m,n)_x$. Use of thin metal layer results in coupling of SPP modes at the top and bottom interfaces resulting in symmetric and antisymmetric modes. Thus, modes with subscript "A" are anti-symmetric and those with "S" are symmetric modes. Modes with subscript "d" are Rayleigh anomalies [19]. While for φ ~0° and φ ~90° orientations (not shown) we see the flat dispersion modes, for all azimuthal angles we see the clear anti-crossing signatures. In Fig. 2 anti-crossings are marked by circles with the zoomed in region shown on the right hand side. In the following we give a model to calculate the anti-crossing width and its dependence on the azimuthal angle.

#186524 - $15.00 USD Received 7 Mar 2013; revised 16 May 2013; accepted 16 May 2013; published 23 May 2013

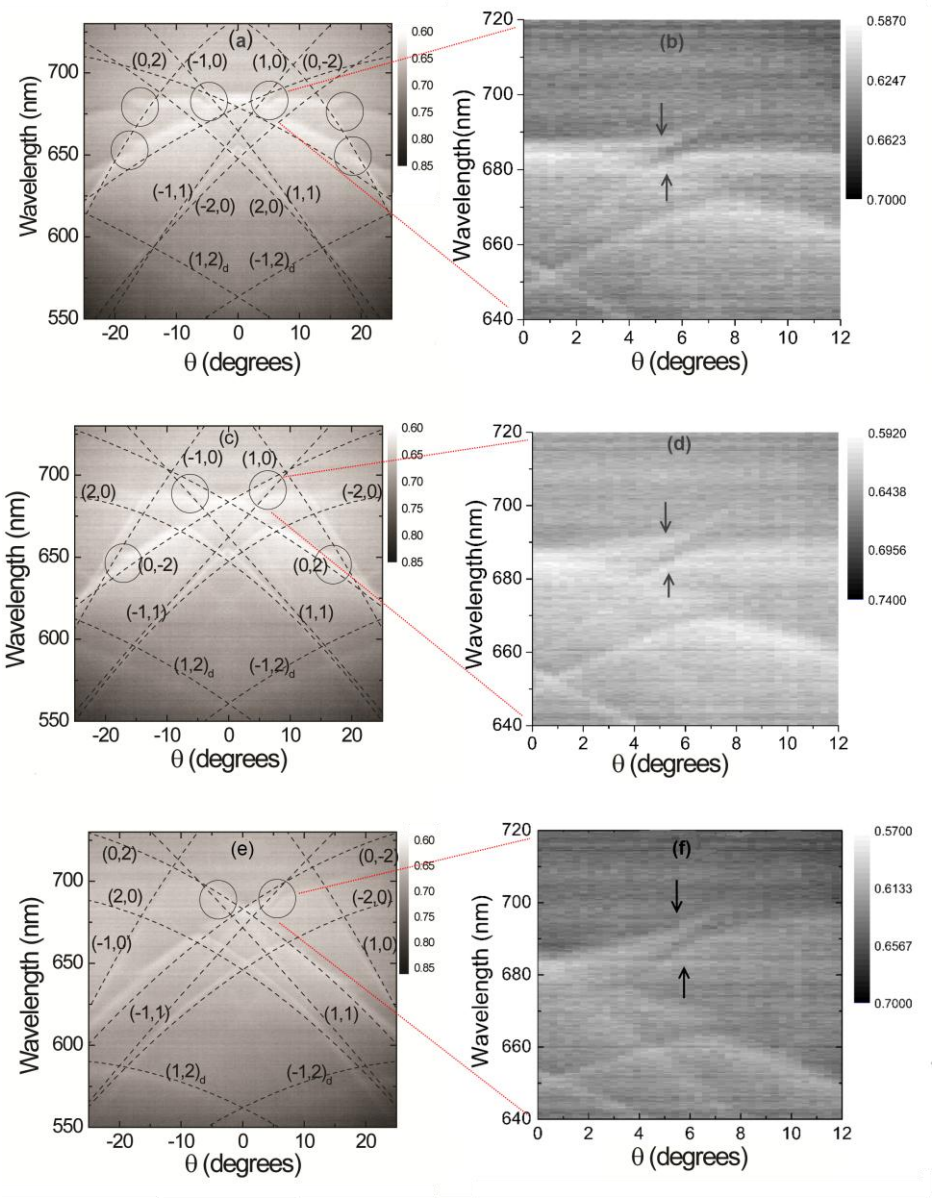

Fig. 2. Measured surface plasmon dispersion for different azimuthal angles is shown as grey scale plots. (a) φ = 15°, (c) φ = 30° (e) φ = 45°. (b), (d) and (f) show zoomed in region with arrows pointing to the anti-crossing site. Contours in lighter shade are the plasmon absorption related transmission dips in the spectra. Dashed lines are calculated grating coupled plasmon mode dispersions. Different modes are labeled. Anti-crossing sites have been marked by circles.

4. Coupled mode theory for calculating anti-crossing width

Coupled mode theory is well known for the orthogonal set of waveguide modes, gratings and other systems [22, 23]. Briefly, when one of the modes locally modifies the dielectric constant then this perturbation induces coupling between different orthogonal modes. In such a picture for the slab waveguide geometry (infinite in x- and y-directions and finite in z-direction) for modes propagating along x-direction, the in-plane and out-of-plane coupling

#186524 - $15.00 USD Received 7 Mar 2013; revised 16 May 2013; accepted 16 May 2013; published 23 May 2013

constants are well known. For 1-D metal grating structure, such a model has been applied recently [24]. We apply the coupled mode theory to the three layer structure with 2D pattern on top by the following procedure. We first calculate the field expressions for the plasmon (surface) modes possible in a 3-level structure and get the expressions for coupling constants for non-collinearly coupled modes. In the 2nd step, we consider the effect of 2D dielectric pattern on top by introducing the relevant k components. By this, we consider only the grating coupled plasmon modes and their coupling.

In the first step, we consider the 3-level structure and the relevant expressions for the TM polarization components (E^x, H^y, and E^z) and calculate the coupling constants. For a three layer system with a thin metal film sandwiched between dielectric materials, solutions to Maxwell's equations with appropriate boundary conditions at the interfaces for TM polarized wave are well known [25]. In the three regions, (in the top dielectric, in the metal and in the bottom dielectric), expressions for the three relevant field components (H^y, E^z and E^x) are in 3 unknown constants. We simplify these equations and write them in terms of a single constant which is solved for by using the power normalization relation,

$$\frac{1}{4}\iint (E_\alpha^{t*} \times H_\beta^t + E_\beta^t \times H_\alpha^{t*}) dydz = \pm\delta_{\alpha\beta}\cos\phi \tag{1}$$

where the integration extends into all the three layers along z-axis and φ is the azimuthal angle with respect to the x-axis. In this case, when $\mathrm{E}(\mathrm{r}) = \sum_\beta \mathrm{A}_\beta(\mathrm{x})\mathrm{E}_\beta(\mathrm{y},\mathrm{z})\mathrm{e}^{\mathrm{ik}_\beta \mathrm{x}}$ is the total field summed over all modes, where A_β governs the evolution of the field. When two of the TM modes are coupled, the in-plane and normal to plane coupling constants are given similar to the overlap integrals [26].

In the 2nd step, we extend the model to the present structure of a three layer system with a 2-D shallow grating on top by considering a periodic perturbative correction to the dielectric constant in the x-y plane. The periodic function can be Fourier expanded as,

$$\Delta\varepsilon(\mathrm{x},\mathrm{y}) = \sum\nolimits_{\mathrm{mn}} \Delta\varepsilon_{\mathrm{mn}} \mathrm{e}^{-\mathrm{imK_x x}} \mathrm{e}^{-\mathrm{inK_y y}} \tag{2}$$

where $K_x = 2\pi/a_x$ and $K_y = 2\pi/a_y$ with a_x and a_y being the periodicities in the x and y directions, respectively. On substituting this in the field propagation equation, it reduces to,

$$\frac{\mathrm{dA}_\alpha(\mathrm{x})}{\mathrm{dx}} = -\mathrm{i}\sum\nolimits_{\mathrm{mn}} \mathrm{K}_{\alpha\beta}^{\mathrm{mn}} \mathrm{A}_\beta(\mathrm{x}) \mathrm{e}^{-\mathrm{i}(\mathrm{k}_\beta + \mathrm{mK_x} - \mathrm{k}_\alpha)\mathrm{x}} \tag{3}$$

where the transverse and the in-plane coupling constants for two interacting modes, α and β, are given by,

$$\begin{aligned} \mathrm{K}_{\mathrm{TM}\alpha\beta}^{\mathrm{mn,t}} &= \frac{\omega\varepsilon_0}{4}\iint \mathrm{E}_\alpha^{\mathrm{Z}*} \Delta\varepsilon_{\mathrm{mn}} \mathrm{e}^{-\mathrm{inK_y y}} \mathrm{E}_\beta^{\mathrm{z}} \mathrm{dydz} \\ \mathrm{K}_{\alpha\beta}^{\mathrm{mn,xy}} &= \frac{\omega\varepsilon_0}{4}\left\{\iint (\mathrm{E}_\alpha^{\mathrm{x}*} \Delta\varepsilon_{\mathrm{mn}} \mathrm{e}^{-\mathrm{inK_y y}} \mathrm{E}_\beta^{\mathrm{x}}) \cos(\phi_\alpha - \phi_\beta) \mathrm{dydz}\right\} \end{aligned} \tag{4}$$

where φ_α and φ_β are the angles made by the propagation vector of each of the waves with the x-axis and E^x is the electric field component along the propagation direction of each mode. The total coupling constant is the sum of the transverse and in-plane coupling constants. Next we calculate the specific k values allowed by the sample and excitation geometry to find the coupling between coplanar SPP modes. For the three layer system with appropriate boundary conditions when we invoke continuity of the field and its derivative at each interface, we get the SPP dispersion relation given by [25],

$$\tan\mathrm{h}(k_1 t) = -\frac{\varepsilon_1 k_1 (\varepsilon_2 k_3 + \varepsilon_3 k_2)}{(\varepsilon_2 \varepsilon_3 k_1^2 + \varepsilon_1^2 k_2 k_3)} \tag{5}$$

#186524 - $15.00 USD Received 7 Mar 2013; revised 16 May 2013; accepted 16 May 2013; published 23 May 2013

where $k_j^2 = k^2 - k_0^2 \varepsilon_j$, j = 1, 2, 3. The k values in this are obtained from Eq. (6) below which gives the possible momenta allowed by the top 2D dielectric pattern.

$$k_{in-plane} = \sqrt{(k_0 \sin\theta\cos\phi \pm \frac{m2\pi}{a_x})^2 + (k_0 \sin\theta\sin\phi \pm \frac{n2\pi}{a_y})^2} \quad (6)$$

The first term in the square root is the k_x component and the second term is the k_y component. For given structure (that is, a_x and a_y) and the measurement geometry (θ, φ), we find the $k_{in\text{-}plane}$ values satisfying both Eq. (5) and Eq. (6) simultaneously. We calculate the coupling constant between two such resonant modes A1(x) and A2(x) given by,

$$\begin{aligned} A1(x) &= A_\alpha(x) e^{i(k_\beta - k_\alpha + mKx)x} \\ A2(x) &= A_\beta(x) e^{-i(k_\beta - k_\alpha + mKx)x} \end{aligned} \quad (7)$$

We solve simultaneously the coupled differential equations (given by Eq. (7)) for these two modes in order to get the splitting due to the coupling. For perfect phase matching i.e. when $k_\alpha = k_\beta + mK_x$, splitting comes out to be $\Delta = 2K_{\alpha\beta}$ in the k_x component. It may be seen from Eq. (4) that the azimuthal angle φ gives control on the coupling strength.

In Fig. 2, we can observe anti-crossing feature between different modes and that the splitting related to the anti-crossing changes with φ. It has been shown earlier that the splitting in the energy and momentum could occur due to conservative and dissipative coupling, respectively [24].

As an example, we consider the case of interaction of (0,2) and (1,1) plasmon modes and how the interaction strength changes with φ. The theoretical values of the splitting have been calculated using Eqs. (4)-(7) which are compared with the measured values in Table 1 as a function of φ.

Table 1. Comparison of measured and calculated split gap for various azimuthal angles.

Angle φ (degrees)	Experimental *K*-splitting $\Delta \pm 0.002$ (μm^{-1})	Calculated *K*-splitting Δ(μm^{-1})
15	0.043	0.047
30	0.149	0.156
45	0.128	0.133
60	0.048	0.054

5. Conclusion

In summary, we have shown the anti-crossing of grating (2D patterned top dielectric) coupled propagating plasmon modes at unpatterned dielectric-metal-dielectric structure due to in-plane coupling. Coupled mode theory for in-plane propagating plasmons, with the sample and measurement geometry considered, shows that the coupling strength and thus the anti-crossing width are azimuthal angle dependent. A good match with the measured and calculated split gap width for in-plane coupled plasmon modes for different azimuthal angles shows that the in-plane coupling strength can be controlled by the azimuthal angle.

#186524 - $15.00 USD Received 7 Mar 2013; revised 16 May 2013; accepted 16 May 2013; published 23 May 2013